



Screening for Highly Transduced Genes in *Staphylococcus aureus* Revealed Both Lateral and Specialized Transduction

 Janine Zara Bowring,^a Yue Su,^a Ahlam Alsaadi,^a Sine L. Svenningsen,^b  Julian Parkhill,^c  Hanne Ingmer^a

^aDepartment of Veterinary and Animal Sciences, University of Copenhagen, Copenhagen, Denmark

^bDepartment of Biology, University of Copenhagen, Copenhagen, Denmark

^cDepartment of Veterinary Medicine, University of Cambridge, Cambridge, United Kingdom

ABSTRACT Bacteriophage-mediated transduction of bacterial DNA is a major route of horizontal gene transfer in the human pathogen, *Staphylococcus aureus*. Transduction involves the packaging of bacterial DNA by viruses and enables the transmission of virulence and resistance genes between cells. To learn more about transduction in *S. aureus*, we searched a transposon mutant library for genes and mutations that enhanced transfer mediated by the temperate phage, $\phi 11$. Using a novel screening strategy, we performed multiple rounds of transduction of transposon mutant pools selecting for an antibiotic resistance marker within the transposon element. When determining the locations of transferred mutations, we found that the screen had selected for just 1 or 2 transposon mutant(s) within each pool of 96 mutants. Subsequent analysis showed that the position of the transposon, rather than the inactivation of bacterial genes, was responsible for the phenotype. Interestingly, from multiple rounds, we identified a pattern of transduction that encompassed mobile genetic elements as well as chromosomal regions both upstream and downstream of the phage integration site. The latter was confirmed by DNA sequencing of purified phage lysates. Importantly, transduction frequencies were lower for phage lysates obtained by phage infection rather than induction. Our results confirmed previous reports of lateral transduction of bacterial DNA downstream of the integrated phage but also indicated a novel form of specialized transduction of DNA upstream of the phage. These findings illustrated the complexity of transduction processes and increased our understanding of the mechanisms by which phages transfer bacterial DNA.

IMPORTANCE Horizontal transfer of DNA between bacterial cells contributes to the spread of virulence and antibiotic resistance genes in human pathogens. For *Staphylococcus aureus*, bacterial viruses play a major role in facilitating the horizontal transfer. These viruses, termed bacteriophages, can transfer bacterial DNA between cells by a process known as transduction, which despite its importance is only poorly characterized. Here, we employed a transposon mutant library to investigate transduction in *S. aureus*. We showed that the genomic location of bacterial DNA relative to where bacteriophages integrated into that bacterial genome affected how frequently that DNA was transduced. Based on serial transduction of transposon mutant pools and direct sequencing of bacterial DNA in bacteriophage particles, we demonstrated both lateral and specialized transduction. The use of mutant libraries to investigate the genomic patterns of bacterial DNA transferred between cells could help us understand how horizontal transfer influences virulence and resistance development.

KEYWORDS *Staphylococcus aureus*, bacteriophages, gene transfer, mobile genetic elements, phages, transducing particles, transduction, transposons

S. *aureus* is a Gram-positive opportunistic pathogen that causes a wide range of diseases in humans. It can become resistant to a variety of antibiotics like methicillin, tetracycline, and vancomycin, and resistance is limiting treatment options (1, 2). The

Editor Joanna B. Goldberg, Emory University School of Medicine

Copyright © 2022 Bowring et al. This is an open-access article distributed under the terms of the [Creative Commons Attribution 4.0 International license](https://creativecommons.org/licenses/by/4.0/).

Address correspondence to Hanne Ingmer, hi@sund.ku.dk.

The authors declare no conflict of interest.

Received 14 December 2021

Accepted 8 January 2022

Published 9 February 2022

staphylococcal genome is highly plastic, largely due to horizontal gene transfer mediated by mobile genetic elements (MGEs), such as staphylococcal pathogenicity islands (SaPIs), plasmids, and phages (3–5). Phage-mediated transduction appears to be an important route of gene transfer (4, 6). Transduction is a process whereby some phages can package bacterial DNA at a low frequency and transfer this DNA between cells (6, 7). Transducing phages are often temperate because they can both be integrated into the bacterial genome as prophages (lysogeny) or be lytic. Transduction can occur through several different mechanisms namely, generalized, specialized, and lateral transduction. In *S. aureus*, generalized transduction has been used for many years as a genetic tool and recently, the mechanism for lateral transduction was established (8–10). In contrast, we know little about specialized transduction in this organism.

Phage $\phi 11$ is one of the best-characterized staphylococcal phages and is regularly used as a laboratory tool for transferring genes by transduction (11). Phage $\phi 11$ is a *pac*-type phage, meaning that it recognizes a phage '*pac*' site and packages DNA into the capsid in a 'headful' manner, terminating when the capsid is filled with slightly more than the ~ 45 kb phage genome (11, 12). As such, $\phi 11$ can transfer bacterial DNA by generalized transduction when bacterial DNA contains sequences with homology to the phage '*pac*' sites (11, 13, 14).

Lateral transduction is a recently identified form of phage-mediated transduction in both *S. aureus* and *Salmonella* (10, 15). Here, it was found that for some temperate phages, replication begins before excision from the host chromosome leading to the replication and packing of the integrated prophage together with the flanking regions of bacterial DNA. In practice, this has led to transduction of up to 100 kb of bacterial DNA downstream of the prophage with frequencies of 1000-fold higher compared to generalized transduction. The study identified that this effect was unidirectional from the *pac* site and so the region upstream of the phage was not transferred (10).

Specialized transduction occurs when a prophage excises incorrectly from the bacterial chromosome (16–25). Instead of a precise excision of the full phage genome between the att_L and att_R sites, an incomplete portion of the phage excises alongside some of the flanking bacterial DNA either upstream or downstream of the phage. If the phage *pac* site is present, this hybrid DNA will be replicated, packaged into phage capsids, and transduced (16, 18, 21). It is limited to the immediate regions of bacterial DNA flanking a prophage. Specialized transduction mechanisms have been reported for phages infecting several bacterial genera, including *Bacillus*, *Salmonella*, *Pseudomonas*, and *Vibrio* (16, 17, 20, 23). However, literature is absent on specialized transduction by staphylococcal phages.

In a recent publication, DNA short- and long-read sequencing was used to investigate the patterns of bacterial DNA in transducing particles in different genera and species of bacteria (26). The patterns observed indicated that different phages and prophages are either more or less prone to lateral, specialized, or generalized transduction and that the same temperate phage may transduce bacterial DNA differently depending on whether that phage is undergoing lytic infection or lysogenic induction (27).

To understand more about transduction processes in *S. aureus*, we explored a screening methodology that allowed us to identify *S. aureus* transposon mutants that were preferentially transduced from a pool of mutants. We utilized the Nebraska transposon mutant library (NTML) in *S. aureus* strain JE2 (28, 29), infecting pools of 96 mutants with the transducing, lysogenic phage $\phi 11$. From this screen, we anticipated identifying genes that either, when inactivated, promoted transduction or were located within the chromosome in regions transduced at higher rates than elsewhere. We showed that the transposon mutations in the chromosomal regions flanking the phage integration site were transduced at higher rates by both lateral and specialized transduction. This study established a simple screening method that reveals patterns of transduction at the genome level, which can be readily applied to transposon mutant libraries of other bacteria. Remarkably, this study was the first to demonstrate specialized transduction in *S. aureus*.

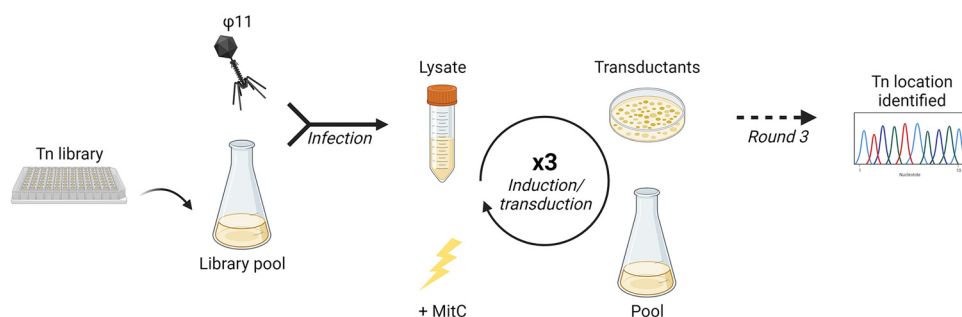


FIG 1 Schematic drawing of the experimental set-up. Depiction of the experimental set-up, indicating the initial pooling and infection by $\phi 11$ of the NARSA transposon mutant library plates, followed by successive rounds of transduction into 8325-4 $\phi 11$, pooling of the resulting transductants, and induction of the $\phi 11$ prophage to produce the next round's lysate. At round three, the resulting transductants were processed as previously described to identify the location of transposon insertion (28, 34). Created with BioRender.com.

RESULTS

Transduction selection preferentially identifies transposon mutations in MGEs and regions flanking prophage $\phi 11$.

Intending to identify genes or mutations that increase transduction frequency, we screened the *S. aureus* JE2 NTML for mutations that were preferentially transduced. To this end we carried out consecutive rounds of transduction on pools of 96 library mutants, infecting these with the transducing temperate phage $\phi 11$ to produce an 'infection' phage lysate containing transducing particles (Fig. 1). We then performed transduction using these lysates with the laboratory strain 8325-4 $\phi 11$, a strain containing only the prophage $\phi 11$, as the recipient. Having the $\phi 11$ prophage present in the recipient, rather than using the phage-less 8325-4, prevented phage superinfection and, thus, increased survival of the transductants. Likewise, the use of this recipient prevented a mixed population of 8325-4 transductants and 8325-4 $\phi 11$ transductants, which would occur using an 8325-4 recipient due to the integration of $\phi 11$. The transfer from JE2 to the 8325-4 $\phi 11$ was conducted to exclude interference from the prophages USA300 ϕ Sa2 and USA300 ϕ Sa3, present in JE2. The core genomes of JE2 and 8325-4 have an identity of 96.6% when aligned using MAUVE, and there was no difference in $\phi 11$ phage titer between 8325-4 and JE2 recipients (Fig. S1).

Transposon-containing transductants in 8325-4 $\phi 11$ were selected for erythromycin resistance, encoded by the transposon. These transductants were pooled and the $\phi 11$ prophage was induced to produce a 'round 1 induction' lysate. The transduction and induction steps were repeated to produce 'round 2' and 'round 3' transduction lysates. Although this was necessary for the selection of highly transduced mutations, this could also have impacted our screen by selecting for transposon mutants of greater fitness. At each stage, the colony forming unit (CFU)/mL and plaque forming unit (PFU)/mL were recorded, and the transduction frequency was calculated, controlling for phage variation ($[\text{CFU}/\text{mL}]/[\text{PFU}/\text{mL}]$; Fig. S2). Importantly, the transduction frequencies showed a significant increase over the three rounds of transduction screening for the seven 96-well plates examined, with the overall mean increasing from -6.8 at infection to -5.7 , -4.5 , and -3.7 at rounds 1, 2, and 3, respectively (Fig. S2).

At the round 3 transduction, we collected 10 colonies from each plate pool and identified the locations of the transposon mutations as described (28). Most pools contained one predominant transposon mutant per biological replicate, leading to ≤ 4 being identified in total for each plate (Fig. 2). For the first biological replicate, only one transposon mutant was identified in 6 of the 7 pools while transposon mutants were identified for plates 1 and 2. Strikingly, half (4 out of 8) of the transposon mutations identified in our initial screen were situated on MGEs (Fig. 2). Of these, one transposon was in a SaPI5 gene, one in the USA300 ϕ Sa2 prophage of JE2 while the other 2 were located in the USA300 ϕ Sa3 JE2 prophage. These MGE-located transposon

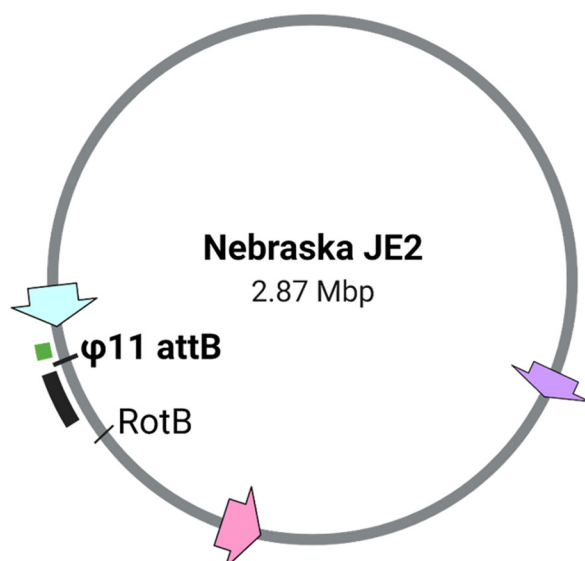


Plate	Gene	Description	Gene number	Replicate	Location
1	vraS	two-component sensor histidine kinase	SAUSA300_1866	1	Upstream of ϕ 11
	-	single-strand binding protein	SAUSA300_1958	1	JE2 Sa3 phage
	serA	D-3-phosphoglycerate dehydrogenase	SAUSA300_1670	2	Downstream of ϕ 11
	-	hypothetical protein	SAUSA300_1706	2	Downstream of ϕ 11
	vraS	two-component sensor histidine kinase	SAUSA300_1866	3	Upstream of ϕ 11
2	-	hypothetical protein	SAUSA300_1868	1	Upstream of ϕ 11
	-	hypothetical protein	SAUSA300_1868	2	Upstream of ϕ 11
	-	hypothetical protein	SAUSA300_1868	3	Upstream of ϕ 11
3	mutY	A/G-specific adenine glycosylase	SAUSA300_1849	1	Downstream of ϕ 11
	mutY	A/G-specific adenine glycosylase	SAUSA300_1849	2	Downstream of ϕ 11
	-	hypothetical protein	SAUSA300_1859	2	Upstream of ϕ 11
	-	hypothetical protein	SAUSA300_1859	3	Upstream of ϕ 11
4	-	hypothetical protein	SAUSA300_0810	1	JE2 SaPI
	hemL	glutamate-1-semialdehyde aminotransferase	SAUSA300_1845	2	Downstream of ϕ 11
	camS	CamS sex pheromone cAM373	SAUSA300_1884	3	Upstream of ϕ 11
5	RusA	putative endodeoxyribonuclease RusA	SAUSA300_1955	1	JE2 Sa3 phage
	-	phiPV083 ORF027-like protein	SAUSA300_1952	2	JE2 Sa3 phage
	RusA	putative endodeoxyribonuclease RusA	SAUSA300_1955	3	JE2 Sa3 phage
6	-	phiSLT ORF 87-like protein, putative DNA-binding protein	SAUSA300_1430	1	JE2 Sa2 phage
	-	conserved hypothetical protein	SAUSA300_1846	2	Downstream of ϕ 11
	-	phi77 ORF069-like protein	SAUSA300_1948	3	JE2 Sa3 phage
7	-	conserved hypothetical protein	SAUSA300_1797	1	Downstream of ϕ 11
	-	phiSLT ORF86-like protein	SAUSA300_1427	2	JE2 Sa2 phage
	-	phi77 ORF031-like protein	SAUSA300_1947	3	JE2 Sa3 phage

FIG 2 Locations of the identified transposon mutations in the JE2 genome. Depiction of NTML JE2 genome (NCBI accession number 007793.1), with MGEs USA300 ϕ Sa2 (pink arrow), USA300 ϕ Sa3 (blue arrow), and JE2 SaPI5 (purple arrow). The ϕ 11 insertion site (att_B) is indicated, as are

(Continued on next page)

mutations were distributed throughout the chromosome (Fig. 2). The other 4 chromosomally situated non-MGE-related transposon mutations clustered around the integration site of the $\phi 11$ (att_B ; Fig. 2). As a prophage, $\phi 11$ integrates into an intergenic region of the 8325 chromosomes with a specific directionality, where the $attL$ was situated at ~ 1.967 Mb and the $attR$ at ~ 1.923 Mb (29). Relative to the $\phi 11$ prophage, 2 of the transposon mutations were situated upstream, but close to, the $\phi 11$ att_B , while the other 2 were located downstream of this site. For subsequent biological replicates, the final transduction plate colonies were pooled for DNA extraction and transposon location identification, in most cases giving one predominant transposon mutant (Fig. 2). The transposon mutations identified were in some cases identical to the first replicate, while all others were in the same regions of either MGEs or upstream and downstream of the $\phi 11$ att_B . To check the impact of fitness on our screen, we performed growth curves on two of the transposon mutants identified (Tn_1868 and Tn_1849) together with two mutants that were included in the pool but not found in the screen (Tn_1799 and Tn_1883) as well as 8325-4 and 8325-4 $\phi 11$ controls (Fig. S3). There were no significant differences in doubling the time between the screen-identified mutants and the nonidentified ones (Table S3). Therefore, we hypothesized that we were identifying transposon mutations that were preferentially transduced due to either induced MGE mobility or lateral and specialized transduction.

Transposon mutants upstream and downstream of $\phi 11$ have an increased transduction frequency. The chromosomal transposon mutants clustering around the $\phi 11$ att_B interested us as potential incidents of specialized or lateral transduction (replicate 1: SAUSA300_1866, SAUSA300_1868, SAUSA300_1849, and SAUSA300_1797). Therefore, we transduced these individual transposon mutations into 8325-4 $\phi 11$ and confirmed by multiplex PCR targeting the phage integrases that none of the JE2 endogenous phages had been transferred (30). Using these ‘clean background’ strains, we confirmed that the transduction frequencies in the 4 chromosomal transposon mutants were higher than our 8325-4 $\phi 11$ $rotB::erm$ transposon control. The $rotB$ transposon mutant has a wild-type phenotype in respect to bacterial growth and transduction, and $\phi 11$ should only transfer this transposon mutation by generalized transduction based on its position in the 8325 genomes (1.794 Mb; Fig. 2). All transposon mutants had significantly higher transduction frequencies than the $rotB$ control (Fig. 3). The initial data (CFU/mL and PFU/mL) for these experiments can be seen in Fig. S4 and a schematic showing the locations of the transposon mutants used for Fig. 3 to 7 can be observed in Fig. S5.

Transposon mutations downstream of the $\phi 11$ integration site are transferred by lateral transduction. Next, we defined the type of transduction occurring with these 4 chromosomal transposon mutants. Lateral transduction occurs in bacterial DNA up to 100 kb downstream of a laterally transducing prophage based on the pac site encoded by that phage. In the case of $\phi 11$, the pac site was in the small terminase gene and this meant that the region downstream of the att_R (< 1.923 Mb) was transferred by lateral transfer while the region upstream of the att_L (> 1.967 Mb) was not (11, 13). Therefore, we hypothesized that the downstream transposon mutations could be transduced laterally. To establish whether the higher transduction frequencies observed in the mutants with transposons located downstream of $\phi 11$ were due to the effects of the specific transposon insertions or the more general effect of lateral transduction, we investigated other transposon mutants from the same region of DNA. We used three different mutants where the transposon was located downstream of the prophage but had not been identified by the replicate 1 screen

FIG 2 Legend (Continued)

the upstream and downstream regions flanking the att_B (green and black bars) and the position of the Tn_1868 control. The table shows the gene in which the transposon was inserted for each identified mutant. ‘Plate’ refers to the plate of the pooled 96 mutants (see Table S1 for NARSA equivalent), ‘replicate’ refers to which biological replicate screen the mutation was identified in, ‘location’ identifies whether the transposon insertion was in an MGE-situated gene or the chromosome (Chr). Upstream and downstream refer to the position of the gene relative to the $\phi 11$ prophage insertion, using the prophage directionality (eg. downstream = downstream of the att_R , upstream = upstream of the att_L). Locations are color-coordinated with the genome map regions.

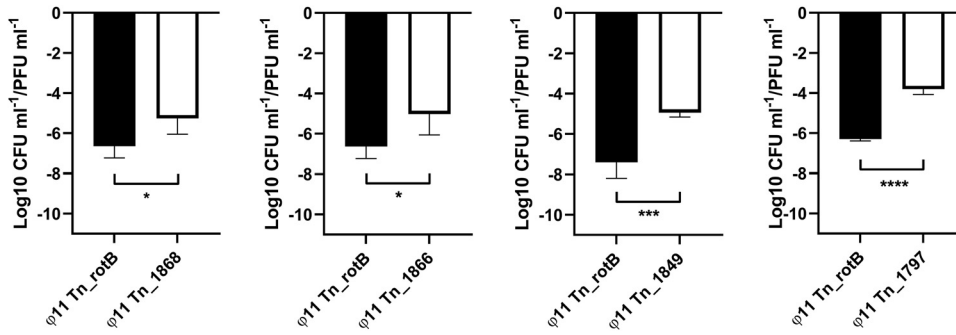


FIG 3 The transduction frequency of the transposon mutants located upstream and downstream of the $\phi 11$ integration site. Graphs showing the transduction frequency (log-transformed CFU mL⁻¹/PFU mL⁻¹) for each mutant compared with Tn_rotB (mean and SD, 4 biological replicates). Unpaired t tests were performed and *P* values from left to right were 0.0312*, 0.0346*, 0.0008***, <0.0001****.

(Tn_1799, Tn_1843, and Tn_1852; Tn_1852 was subsequently identified in a later screen). We measured the transduction frequency of these transposon mutants in 8325-4 $\phi 11$ following induction. All three had a significantly higher transduction frequency than the Tn_rotB control (Fig. 4) and were comparable to the Tn_1849 and Tn_1797 mutants.

Because these mutants had a high transduction frequency similar to that of the mutants from the screen, it suggested that lateral transduction was responsible. Because lateral transduction only occurred when a prophage was induced, we tested the transduction frequency of both the original mutants and these 'neighboring' mutants following infection where lateral transduction could not occur. The transposon mutants in the JE2 background were infected with $\phi 11$ and the transduction frequency of the resulting lysate was established. The transduction frequencies of all the transposon elements located downstream of $\phi 11$ were higher than the Tn_rotB control (Fig. 5A and B). However, these transduction frequencies were significantly reduced for Tn_1843, Tn_1852, and Tn_1797 compared to the previous induction-linked frequencies (Fig. 5C to E). Furthermore, Tn_1799 and Tn_1849 both showed lower transduction frequencies following infection, although these differences were not significant. This showed that lateral transduction was the main cause of the increased transduction frequencies downstream of the $\phi 11$ integration site.

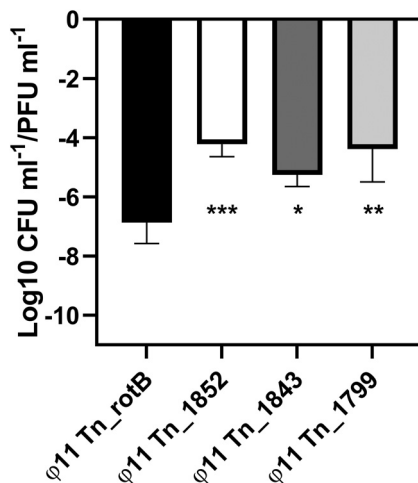


FIG 4 The transduction frequency of chromosomal regions downstream of the $\phi 11$ integration site was not observed in the original transduction screen. The graph shows the CFU/PFU transduction frequency (mean and SD, 4 replicates) for the induced lysate of each downstream mutant compared with Tn_rotB control. A one-way ANOVA was performed with Dunnett's multiple-comparison test comparing the mean of the Tn_rotB control with each mutant's mean, and *P* values from left to right were 0.0006***, 0.0203*, and 0.0010**.

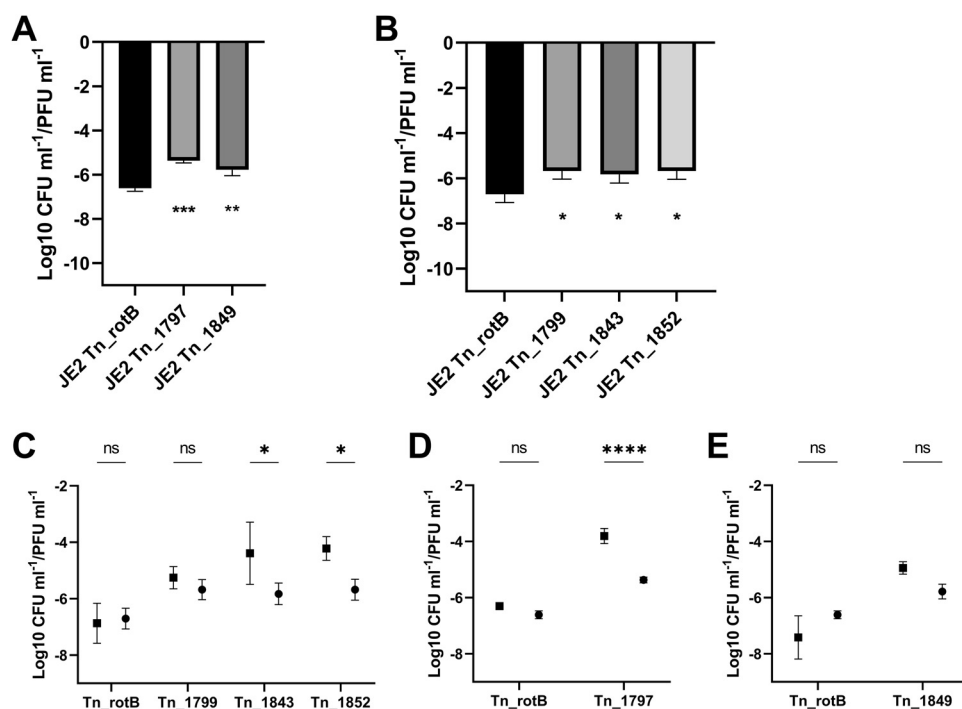


FIG 5 Lateral transduction of JE2 transposon mutations downstream of $\phi 11$. (A) The CFU/PFU transduction frequency following infection with $\phi 11$ for each JE2 downstream mutant from the initial screen compared with JE2 Tn_rotB (Tn inserted into SAUSA300_1797 and SAUSA300_1849, respectively). *P* values for a one-way analysis of variance (ANOVA) with Dunnett's multiple-comparison test were 0.0003*** and 0.0027** (left to right). (B) The CFU/PFU transduction frequency for the control JE2 Tn_rotB and the other JE2 Tn mutants downstream of the $\phi 11$ integration site following infection with $\phi 11$ (Tn inserted into SAUSA300_1799, SAUSA300_1843, and SAUSA300_1852, respectively.) *P* values for a one-way ANOVA with Dunnett's multiple-comparison test were 0.0233*, 0.0476*, and 0.0233* (left to right). All values shown were log-transformed and showed the means and SD from the 3 replicate values. (C to E) The CFU/PFU transduction frequency following either infection or induction with $\phi 11$. (C) Comparison of the induction (square) and infection (circle) transduction frequencies of the neighboring transposon mutants and the Tn_rotB control, showing the means and standard deviation (SD). *P* values for a two-way ANOVA with Sidak multiple-comparison test were 0.9944^{ns}, 0.8400^{ns}, 0.0212*, and 0.0190* left to right. (D and E) Comparison of the induction (square) and infection (circle) transduction frequencies of the Tn_rotB control together with Tn_1797 and Tn_1849, respectively. *P* values for a two-way ANOVA with Sidak multiple-comparison test were (D) 0.0830^{ns} and <0.0001**** (E) 0.0874^{ns}, and 0.0747^{ns}.

Transposon mutations upstream of the $\phi 11$ integration site are transferred by specialized transduction. To establish whether the genes located upstream and close to the $\phi 11$ integration site were transduced at higher frequencies due to gene-specific effects or because of specialized transduction, additional transposon mutants from this region were examined. The mutants in the same region as Tn_1866 and Tn_1868 showed comparable transduction frequencies, while the mutant with the transposon element furthest from the phage integration site (62 kb upstream) showed a gradual reduction in transduction frequency, albeit notably higher than the Tn_rotB control (Fig. 6; Tn_1865, Tn_1883, and Tn_1898 versus Tn_1916, respectively).

Furthermore, when antibiotic resistances from the original JE2 transposon mutants were transduced following $\phi 11$ infection, the transduction frequencies were lower and not significantly different to the Tn_rotB control (Fig. 7). Given that specialized transduction did not occur during infection, these results suggested that specialized transduction was occurring in the region immediately upstream of the $\phi 11$ and caused the higher levels of transduction seen. Indeed, by using primers annealing within the NTML transposon (Martn-ermR) and the $\phi 11$ phage (phi11-direction-3f) it was possible to amplify products from induced lysates of 8325-4 $\phi 11$ Tn_1866 and 8325-4 $\phi 11$ Tn_1868 (Fig. 8). This indicated that some transducing particles in these lysates contained the upstream regions of bacterial DNA alongside the 5'-end region of the phage genome, which would be expected for specialized transduction.

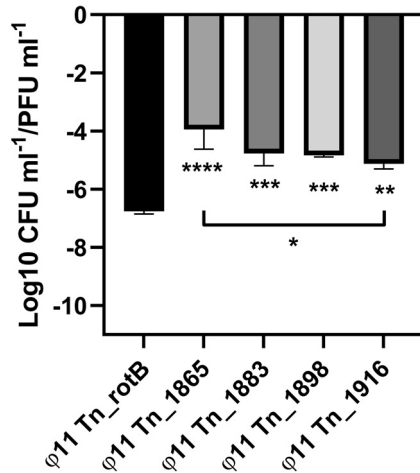


FIG 6 The transduction frequency of transposon mutations from the chromosomal region upstream of the $\phi 11$ integration site that was not selected in the original transduction screen. The graph shows the CFU/PFU transduction frequency for each upstream mutant compared with Tn_rotB. A one-way ANOVA was performed with Tukey multiple-comparison test comparing the means. Comparison of the Tn_rotB control with each mutant mean gave P values from left to right of <0.0001 ****, 0.0005 ***, 0.0006***, and 0.0022*. An additional comparison of the Tn mutant closest to the $\phi 11$ insertion site (Tn_1865) to the one furthest away (Tn_1916) is indicated by the black line, with a P value of 0.0188*. All values shown were log-transformed and showed the means and SD for 3 biological replicates.

Likewise, when we transduced the Tn_1866 and Tn_1868 transposon mutations into an 8325-4 as opposed to 8325-4 $\phi 11$ recipient, the percentage of 8325-4 recipients that by PCR were also positive for the Sa5 Int encoded by $\phi 11$ was significantly higher than observed when examining cells where the Tn_RotB had been transduced (Fig. S6). This would be expected with specialized transduction where the majority of transductant DNA injected into a new recipient cell would recombine with an integrated coinfecting phage and, therefore, selecting for a higher proportion of lysogenic recipient cells (18).

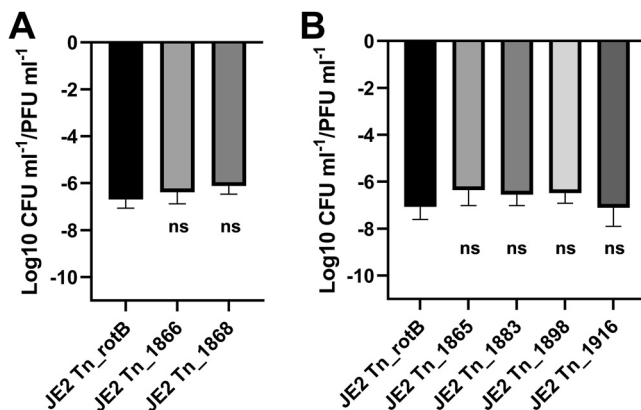


FIG 7 The transduction frequency of upstream-located JE2 transposon mutations following infection with $\phi 11$. (A) The CFU/PFU transduction frequency for the control JE2 Tn_rotB and the different screen-identified Tn mutants upstream of the $\phi 11$ integration site following infection with $\phi 11$ (Tn inserted into SAUSA300_1866 and SAUSA300_1868, respectively). P values for a one-way ANOVA with Dunnett's multiple-comparison test were 0.5807^{ns} and 0.2225^{ns}. (B) The CFU/PFU transduction frequency for the control JE2 Tn_rotB and the different neighboring Tn mutations upstream of the $\phi 11$ integration site following infection with $\phi 11$ (Tn inserted into SAUSA300_1865, SAUSA300_1883, SAUSA300_1898, and SAUSA300_1916, respectively). P values for a one-way ANOVA with Dunnett's multiple-comparison test were 0.4197^{ns}, 0.6682^{ns}, 0.5882^{ns}, and 0.9999^{ns} (left to right). All values shown were log-transformed and showed the means and standard deviation from the 3 replicate values.

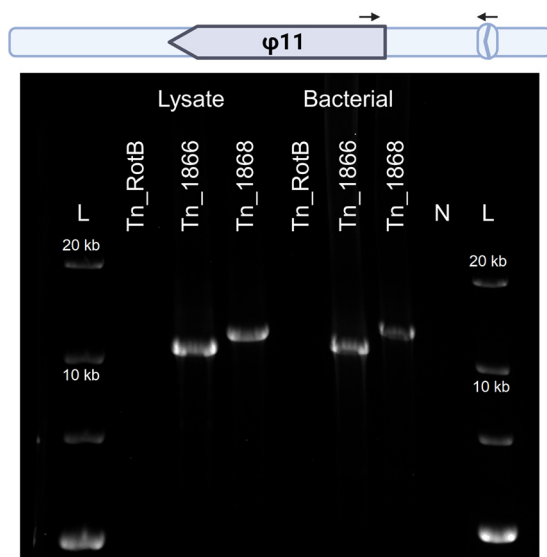


FIG 8 Amplified specialized transduction fragments from precipitated phage DNA. A 0.6% agarose gel showing the PCR products of a long-range amplification using TaKaRa LA polymerase. Diagram indicates the position of the $\phi 11$ phage genome in relation to the transposon mutations and black arrows indicate the primer positions. The reverse primer anneals to the erythromycin resistance gene present in all the transposon mutations. Templates, from left to right, were DNA extracted from precipitated phage capsids from an induced lysate of 8325-4 $\phi 11$ Tn_RotB, an induced lysate of 8325-4 $\phi 11$ Tn_1866, an induced lysate of 8325-4 $\phi 11$ Tn_1868 or bacterial DNA from a culture of 8325-4 $\phi 11$ Tn_rotB, 8325-4 $\phi 11$ Tn_1866, and 8325-4 $\phi 11$ Tn_1868. N indicates no template. The expected size for region $\phi 11$ to Tn_1866 was ~ 10.6 kb and ~ 11.7 kb for region $\phi 11$ to Tn_1868. Three biological replicates were performed, including induction, precipitation, DNA extraction, and PCR, and the above gel is representative. Primers Martn-ermR and Phage direction-3f were used for all templates (Table S2).

Regions identified from the preferentially transduced transposon elements are packaged at higher frequencies than the rest of the genome. To support our genetic screen, we sequenced phage $\phi 11$ lysates from mitomycin C induced 8325-4 $\phi 11$ lysogen to directly identify bacterial DNA packaged in phage capsids. Fig. 9 shows the mapping of the reads to 8325-4, thus removing reads mapping to the phage and allowing the lower frequency reads that mapped to the bacterial genome to be seen. Regions of elevated coverage were identified by dividing the genome into 13.5 Kbp bins and comparing the average coverage for each bin. The region between 1.09 and 2.01 Mbp was identified as the single region with significantly elevated coverage, with a mean depth overall of 5.6. This corresponded to the regions upstream and downstream of the $\phi 11$ att_B (indicated by the red line), supporting our screening data in which the identified mutants were clustered in this same region. The rest of the genome showed only the baseline level of reads mapping, with an average mean depth overall of 1.1. The pattern of the downstream bacterial DNA indicates that lateral transduction may be responsible, with a gradual reduction of mapped reads from high numbers near to the att_B, decreasing further away from the attachment site. Lateral transduction has been shown to taper off in this fashion, while still facilitating the transfer of ~ 200 kb of downstream bacterial DNA (10). Here, we see elevated read mapping as far away as 798 kb downstream from the att_B site (mean depth 1093501 to 1107000 bp, 2.6). The read alignments of the upstream bacterial DNA peak encompass 117 kb of DNA upstream of the att_B (mean depth 1998001 to 2011500 bp, 5.6). These reads could represent the effect of specialized transduction following the incorrect excision of the phage, albeit representing a larger region than one would expect with a phage genome length of ~ 45 kb. In addition, there was mismapping of phage reads forming a large peak left of the att_B and a single large peak to the right of the att_B, mapped to the ribosomal operon containing three ribosomal genes encoding 5S, 23S, and 16S rRNA, these were excluded from the analysis.

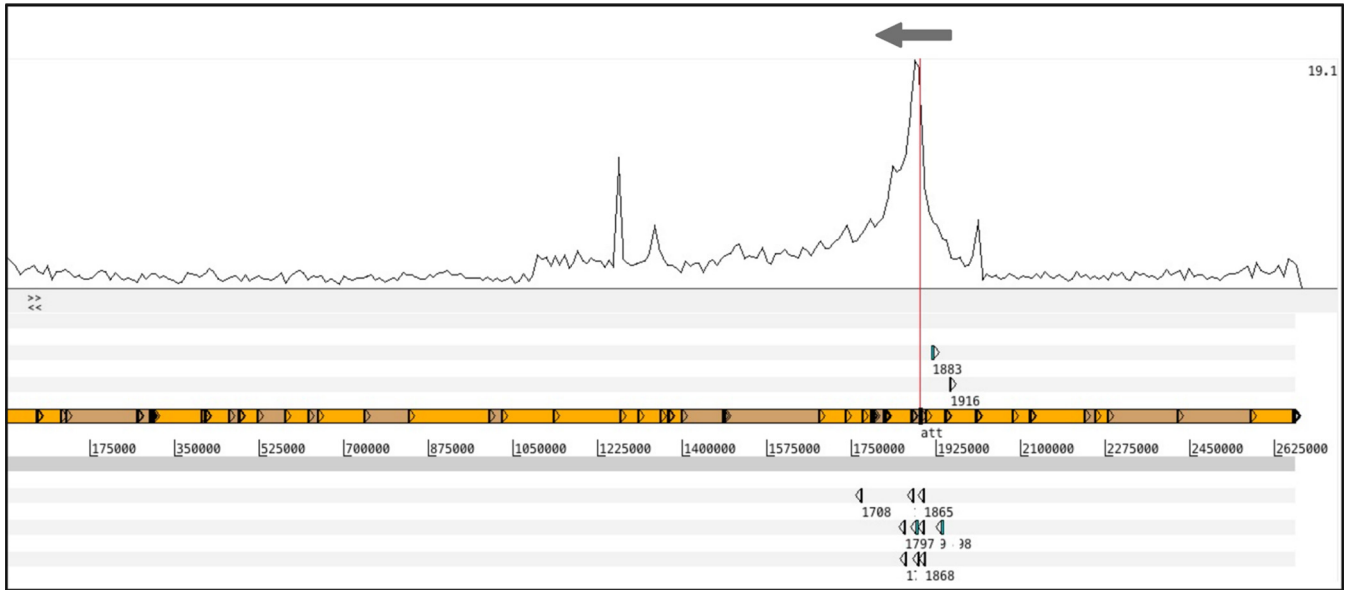


FIG 9 Mapping of lysate-derived DNA to the 8325-4 chromosome. The top graph shows read mapping to the 8325-4 chromosome. Elevated coverage was identified between 1093501 and 2011500 bp with an independent *t* test performed to compare the mean read mapping between the high coverage and the rest of the genome, *P* value <0.0001****. One-sample *t* tests were also performed to compare the mean read mapping at the boundaries of the region of elevated coverage. Bin 82 (1093501 to 1107000 bp) was compared against the mean of bins 1 to 81 (1 to 1093500 bp), *P* value <0.0001****, and bin 149 (1998001 to 2011500 bp) against the mean of bins 150 to 198 (2011501 to 2668682 bp), *P* value <0.0001****. The red line indicates the site of insertion of ϕ 11 in the lysogen, with the gray arrow indicating the orientation of the phage. Beneath this is the six-frame translation (top three and bottom three lines) where the genes referred to in this study are represented by blue boxes, with the NTML gene numbers included. The central two lines represent the forward and reverse DNA strands, with the concatenated assembly contigs identified with alternating orange and brown boxes. The narrow peak of read mapping to the left of the insertion site is caused by mismapping of phage reads, and the narrow peak to the right is caused by multiple mapping to an rRNA operon.

Based on our observations that these upstream regions were being transduced alongside the phage genome (Fig. 8), together with the unexpectedly large regions of elevated read mapping of these upstream regions (Fig. 9), we hypothesized that the transduction of this region was more complex than the wrongful excision of the prophage. Traditionally specialized transduction is defined as misexcision where nonhomologous recombination of the incomplete phage and bacterial flank leads to their circularization and *pac*-based packaging. This would limit specialized transduction to the flanking regions less than a phage genome-length (~45 kb, plus redundancy) away from either the *att_L* or *att_R*. However, here we identified elevated reads mapping and increased transduction frequencies up to 117 kb upstream of the *att_B* (Fig. 6 and 9, respectively). Interestingly, outside the region of elevated reads, the transduction frequencies were not significantly different from the Tn_RotB control (Fig. S7).

We hypothesized that the extended regions of elevated transduction frequencies could be explained by homologous regions flanking the integrated prophage and upstream region enabling homology-based circularization of this region, including the phage. BLASTn of the nucleotide sequence up to 45 kb downstream of the *att_B* with the upstream region of elevated reads mapping, indicated a 3.1 kb region of 99% identity between a region at the end of the elevated reads mapping and another ~18 kb downstream of the *att_B*. If these regions were circularized it would include the complete prophage genome, which could facilitate packaging of both phage and bacterial DNA from the *pac* gene while integrated into this episome-like circular structure, similarly to the packaging of integrated DNA during lateral transduction. To confirm whether this circularization could occur, primers were designed to amplify the hypothetically circularized region. Following large plasmid extraction, we could amplify the product from both noninduced and induced 8325-4 ϕ 11 (Fig. S8).

DISCUSSION

We described a high-throughput method by which the mobile regions of bacterial genomes can be identified. By screening pooled transposon mutants, we were able to

identify different modes of phage-related horizontal gene transfer, including lateral and specialized transduction. The method could be applied to any strain for which there is a transposon mutant library available. Before our screen, we anticipated obtaining two types of mutants; namely, those where the transposon was placed in a genome location transferred with higher frequency, for example, by lateral transduction and mutants that due to inactivation of a bacterial gene would lead to increased transduction efficacy. The results showed, however, that we primarily obtained mutants belonging to the first category and, in addition, transposon elements that had been inserted into MGEs. Thus, for three of the resulting transposon mutants from the first replicate screen, the transposon element was inserted in phages being endogenous to the JE2 strain, namely, the USA300 ϕ Sa2 and USA300 ϕ Sa3, and these had been transferred to the 8325-4 background. This phage transfer was not unexpected because prophages can be induced by an infecting phage and the 8325-4 strain encodes attachment sites for these phages (11, 12, 31).

For two of the transposon mutants preferentially selected in our first screen, the transposon elements were located downstream of the ϕ 11 attachment site (SAUSA300_1849 and SAUSA300_1797). These mutants displayed high transduction frequencies following induction, compared to a control where the antibiotic resistance marker was located elsewhere in the bacterial genome, and this effect was reduced when the transfer was monitored following phage infection. We concluded that the increased transduction frequency for these mutations was dependent on the induction of an integrated ϕ 11 and that they were transferred by lateral transduction (10). This notion was supported by bacterial DNA sequences obtained from induced phage lysates that indicated extensive packaging of bacterial DNA downstream of the integrated phage. Interestingly, these data implicate lateral transduction at an even greater distance downstream of the att_B site than has previously been suggested (10), with slightly elevated reads mapping up to 798 kb downstream.

It has been shown that temperate phages are capable of both generalized and specialized transduction (16, 32), but specialized transduction had not been reported in *S. aureus* until now. However, for the transposon mutants Tn_1866 and Tn_1868 identified in our screen, the transposon element was located immediately upstream of the ϕ 11 integration site at a distance of 7.6 and 8.7 kb, respectively, thus placing it comfortably within a region where specialized transduction could be expected to occur. The increased transduction frequencies of Tn_1866 and Tn_1868 were eliminated when lysates were created by infection rather than induction, removing the possibility of generalized transduction. Equally, they would not be transferred by lateral transduction, which occurs downstream of the phage *pac* site (10). This left specialized transduction as the remaining, feasible explanation. Indeed, we were able to identify PCR products containing both ϕ 11 and the transposon using precipitated phage lysate from the strains with Tn_1866 and Tn_1868. This indicated that some phage capsids contained both the att_L region of the phage together with the upstream flanking region up to 8.7 kb away. Further, the majority (91% and 86%, respectively) of 8325-4 Tn_1866 and 8325-4 Tn_1868 transductant colonies were positive for the ϕ 11 integrase. For *Salmonella* phage P22 it has been seen that specialized transduction into a recipient bacterium is mediated by recombination with an integrated prophage (15, 18). Therefore, we expect that in our case, specialized transduction may involve recombination between a transducing particle carrying DNA upstream of the phage and a coinfecting phage during infection. These data, support that the upstream genes are transferring through specialized transduction.

The DNA sequencing of the precipitated phage particles from induced 8325-4 ϕ 11 correlated well with the transduction frequencies of our selected transposon mutation strains. As such, we were initially confused by the extended region of elevated reads mapping to 117 kb upstream of the phage attachment site. While the transposon mutations in genes 1866 and 1868 sit well within the region of classical specialized transduction (less than 10 kb upstream of the att_B), the mutation in Tn_1916 is 62 kb

upstream and still showed significantly higher transduction frequencies than the Tn_RotB control. Although this correlated with DNA sequencing, it could not be transferred by classical specialized transduction. Outside of the region indicated by our sequencing data, we no longer saw the higher transduction frequencies. Using the DNA sequencing data, we identified the end of the elevated reads mapping and found that this region had a 3.1 kb homologous region with 99% identity downstream of the phage. We hypothesized and confirmed that this region could recombine and in doing so form a large circle of DNA that would include the complete $\phi 11$ prophage. We speculate that the homologous regions up and downstream of the $\phi 11$ could facilitate a new variation of specialized transduction involving circularization of both prophage and flanking regions. Future work into this interesting phenomenon will look into the molecular mechanism by which such circularization could take place and how it is related to phage replication and packaging.

A limitation of our screen is the coselection for transposon mutants with greater fitness. This may explain why within our pooled mutants we identified a limited number of transposon mutations from the highly transduced regions, even though others were present in the pool. The transposon mutations identified in the screen may well represent those of higher fitness relative to the other highly transduced transposon mutants from that pool.

This study acts as a proof of concept for using transposon mutant libraries to investigate which regions of the bacterial genome are highly mobile. We showed phage transfer, generalized, specialized, and lateral transduction between staphylococcal strains. While the setup employed here was used to identify highly transduced genes and chromosomal locations, it may also reflect what happens over time in the real world. The release of $\phi 11$ from lysogens promotes the acquisition of bacterial DNA by auto-transduction and resulting transductants will, as lysogens, be able to repeat the process (33). Horizontal gene transfer underpins the evolution and adaptability of *S. aureus* and approaches such as the one adopted here will help us increase our understanding of which regions are transferred and how.

MATERIALS AND METHODS

Bacterial strains and growth conditions. Bacterial strains used in this study are listed in Table S1. *S. aureus* strains were grown in tryptic soy broth (TSB) and on tryptic soy agar (TSA) plates (Oxoid) with or without antibiotics as appropriate.

Growth curves. Bacterial growth curves were performed in TSB using the bioscreen C automated microbiology growth curve analysis system. Briefly, overnight cultures were subcultured in TSB to an optical density at 600 nm of 0.01 and 250 μ L plated in each well of the bioscreen C honeycomb 100-well plates. The OD₆₀₀ was recorded every 30 min for 24 h at 37°C with shaking, which was paused 5 s before each read. Growth curves were analyzed using the GrowthCurver R script and the t_gen (or doubling time) was compared between strains.

Bacteriophage titer. Phage titers were performed as previously described (10, 33). Briefly, recipient strains were grown to 0.35 OD₆₀₀ and 100 μ L aliquots of recipient mixed with 100 μ L phage lysate, at different dilutions in phage buffer (10^0 to 10^{-8} ; MgSO₄ 1 mM, CaCl₂ 4 mM, Tris-HCl pH 8 50 mM, NaCl₂ 0.1 M). After 10 min incubation at room temperature, 3 mL of liquid PTA (phage top agar; Oxoid nutrient broth no. 2, agar 3.5% wt/vol) was added and the mixture was poured out on PB plates (phage base; nutrient broth no. 2, agar 7% wt/vol). Plates were incubated at 37°C overnight and plaques were counted.

Bacteriophage transduction. Phage transductions were performed as previously described (10, 33). Briefly, recipient strains were grown to 1.4 OD₆₀₀, 4.4 mM CaCl₂ added, and 1 mL aliquots of recipient mixed with 100 μ L phage lysate, at different dilutions in phage buffer (10^0 to 10^{-4}). After 20 min incubation at 37°C, 3 mL of liquid TTA (transduction top agar; TSA, 50% agar) was added and the mix was poured out on selective TSA plates. Plates were incubated at 37°C for 24 h and colonies were counted.

The transduction frequency was calculated using the CFU/mL divided by the PFU/mL to control for variation between lysates.

Bacteriophage infection and induction. Bacteriophage infection was performed as previously described (33). Briefly, recipient bacteria were grown to 0.15 OD₆₀₀ and centrifuged, before resuspending the pellet in 1:1 TSB and phage buffer. The culture was then infected with phage at a multiplicity of infection (MOI) of 1 and incubated at 30°C, 80 rpm until complete visual lysis, normally after 3 to 4 h. Lysates were then filtered using 0.22 μ M filters and stored at 4°C.

Bacteriophage induction was performed as previously described (10, 33). Briefly, lysogens were grown to an OD₆₀₀ of 0.1 to 0.2 and 2 μ g/mL mitomycin C (Sigma, from *Streptomyces caespitosus*) was added to induce resident prophages. Cultures were then incubated at 30°C, 80 rpm until complete visual lysis. Lysates were filtered using 0.22 μ M filters and stored at 4°C.

NTML transposon transduction screening. One 96-well plate was replicated and grown overnight in selective TSB (erythromycin, 5 μ g/mL) before pooling 10 μ L of each mutant in 100 mL selective TSB in a

500 mL flask. The culture was infected with ϕ 11 (MOI 1) as described. The lysate was then used to transduce the NTML transposons to 8325-4 ϕ 1, as described. The transduction plate of undiluted lysate was harvested, pooled, and grown in selective TSB and the culture was diluted then induced. This lysate was used to transduce into the 8325-4 ϕ 11 recipient a second time, and the transductants were pooled and induced. From the resulting lysate, a third transduction was performed, 10 transductant colonies selected, or all colonies were pooled, and the location of the transposon mutation(s) identified as previously described (28, 34).

DNA sequencing. Preparation of the phage lysates for DNA sequencing was done by precipitating the phage capsids before DNA extraction. For the phage precipitation, DNase (2.5 U/mL, Thermo) and RNase (1 μ g/mL, Sigma) were added to the filtered lysate before incubation at 37°C for 1 h. NaCl₂ (1 M) was added and mixed on the ice at 4°C for 1 h. The lysate was centrifuged at 11,000 \times *g* for 10 min at 4°C and the supernatant was collected, mixed with PEG 8000 (10% wt/vol), before incubation on ice overnight at 4°C. The lysate was centrifuged at 11,000 \times *g* for 10 min at 4°C and supernatant discarded, with falcon tubes dried. The pellet appeared as two vertical white lines and was resuspended in 8 mL phage buffer per 500 mL lysate, with resuspension for 1 h at 4°C. DNA extraction was performed using the MagAttract HMW DNA kit (Qiagen) per the manufacturer's instructions. DNA concentration and absorbance peaks were checked using a Thermo NanoDrop 2000 and a Qubit Flex Fluorometer. A draft genome for 8325-4 was generated by sequencing chromosomal DNA on an Illumina miSeq following the manufacturer's instructions. The sequence was assembled, and the contigs were ordered using the Sanger Institute pipelines (35). Phage lysate DNA was sequenced in the same way, and the resulting reads were mapped to this genome using SMALT (35, 36) and visualized using Artemis (35, 37).

To identify regions of elevated coverage, the genome was split into 198 bins of 13.5 Kbp, and an area of elevated coverage was identified between 1093501 and 2011500 bp, corresponding to bins 82 to 149, after calculating the coverage for each bin. To test whether this region had significantly elevated coverage compared to the rest of the genome, an independent *t* test was performed comparing the coverage observed in these two bin categories. Further statistical analyses were performed to test whether the elevated coverage at the ends of the elevated region remained above the background coverage of the rest of the genome. A one-sample *t* test was performed to compare the mean of the coverage distribution of bins 1 to 81 against bin 82, and another to compare bin 149 with the mean of bins 150 to 198.

DNA methods. General DNA manipulations were performed using standard procedures. Primers used in this study can be found in Table S2. PCRs were performed using DreamTaq Green master mix (2 \times ; Thermo Fisher Scientific) per the manufacturer's instructions. PCRs for identification of transposon locations were performed as previously described (28). PCR products were sequenced at Eurofins MWG Operon.

For identification of prophages in strains, a multiplex PCR for the main integrases of the staphylococcal phages was performed, as previously described (30). Initial screening of colonies was performed using 1 μ L of template from a single colony resuspended in 50 μ L ddH₂O, boiled for 10 min, and on ice for 10 min. Results were confirmed using DNA template (10 ng), extracted using GenElute™ Bacterial Genomic DNA kit as per manufacturer's instructions (Sigma-Aldrich). For integrase checks of transductants, colony PCRs using just the Sa5 Int primers was performed as described above.

For long amplifications, the Takara LA polymerase PCR kit was used per the manufacturer's instructions with the following alteration, a 30 s annealing step was added at 55°C. Templates used were either bacterial DNA extracted with the GenElute™ Bacterial Genomic DNA kit or phage DNA extracted from phage lysates that had been precipitated, as previously described, and extracted using the GenElute™ Bacterial Genomic DNA kit with an extended proteinase K incubation of 1 h (Sigma-Aldrich). Fifty nanograms of the template were used for each PCR. The resulting products were run out on a 0.7% agarose gel at 30 V overnight.

For extraction of the large plasmid-like structures, samples were grown for 1 h, before induction with MitC as described. Samples were taken at the time of induction (T0) and 1 h after induction, with noninduced samples also taken. Fifty milliliters of the culture was taken per sample and prepared as previously described (38), with the amounts doubled and RNase added to the resuspension buffer. Sixty nanograms of the template were used for subsequent PCRs using a DreamTaq polymerase kit.

Statistical analyses. Data analyses were performed in GraphPad Prism 8 software. Specific statistical tests are indicated in the figure legends, where appropriate.

SUPPLEMENTAL MATERIAL

Supplemental material is available online only.

SUPPLEMENTAL FILE 1, PDF file, 1.5 MB.

ACKNOWLEDGMENTS

We thank Evangelos Dimopolous for his help with the analysis of the phage lysate sequencing data. Funding bodies were Olav Thon Foundation, Independent Research Fund, Denmark and Wellcome.

We declare no conflict of interest.

REFERENCES

1. Appelbaum PC. 2006. The emergence of vancomycin-intermediate and vancomycin-resistant *Staphylococcus aureus*. *Clin Microbiol Infect* 12: 16–23. <https://doi.org/10.1111/j.1469-0691.2006.01344.x>.
2. DeLeo FR, Otto M, Kreiswirth BN, Chambers HF. 2010. Community-associated methicillin-resistant *Staphylococcus aureus*. *Lancet* 375:1557–1568. [https://doi.org/10.1016/S0140-6736\(09\)61999-1](https://doi.org/10.1016/S0140-6736(09)61999-1).

3. Goerke C, Wolz C. 2004. Regulatory and genomic plasticity of *Staphylococcus aureus* during persistent colonization and infection. *Int J Med Microbiol* 294:195–202. <https://doi.org/10.1016/j.ijmm.2004.06.013>.
4. Lindsay JA. 2014. *Staphylococcus aureus* genomics and the impact of horizontal gene transfer. *Int J Med Microbiol* 304:103–109. <https://doi.org/10.1016/j.ijmm.2013.11.010>.
5. Martínez-Rubio R, Quiles-Puchalt N, Martí M, Humphrey S, Ram G, Smyth D, Chen J, Novick RP, Penadés JR. 2017. Phage-inducible islands in the Gram-positive cocci. *ISME J* 11:1029–1042. <https://doi.org/10.1038/ismej.2016.163>.
6. Xia G, Wolz C. 2014. Phages of *Staphylococcus aureus* and their impact on host evolution. *Infect Genet Evol* 21:593–601. <https://doi.org/10.1016/j.meegid.2013.04.022>.
7. Deghorain M, Van Melderen L. 2012. The *Staphylococci* Phages Family: an Overview. *Viruses* 4:3316–3335. <https://doi.org/10.3390/v4123316>.
8. Lennox ES. 1955. Transduction of linked genetic characters of the host by bacteriophage P1. *Virology* 1:190–206. [https://doi.org/10.1016/0042-6822\(55\)90016-7](https://doi.org/10.1016/0042-6822(55)90016-7).
9. Zinder ND, Lederberg J. 1952. Genetic exchange in *Salmonella*. *J Bacteriol* 64:679–699. <https://doi.org/10.1128/jb.64.5.679-699.1952>.
10. Chen J, Quiles-Puchalt N, Chiang YN, Bacigalupe R, Fillol-Salom A, Chee MSJ, Fitzgerald JR, Penadés JR. 2018. Genome hypermobility by lateral transduction. *Science* 362:207–212. <https://doi.org/10.1126/science.aat5867>.
11. landolo JJ, Worrell V, Groicher KH, Qian Y, Tian R, Kenton S, Dorman A, Ji H, Lin S, Loh P, Qi S, Zhu H, Roe BA. 2002. Comparative analysis of the genomes of the temperate bacteriophages ϕ 11, ϕ 12 and ϕ 13 of *Staphylococcus aureus* 8325. *Gene* 289:109–118. [https://doi.org/10.1016/S0378-1119\(02\)00481-X](https://doi.org/10.1016/S0378-1119(02)00481-X).
12. Gillaspay AF, Worrell V, Orvis J, Roe BA, Dyer DW, landolo JJ, 2014. The *Staphylococcus aureus* NCTC 8325 Genome, p 381–412. In Fischetti VA, Novick RP, Ferretti JJ, Portnoy DA, Rood JI. (ed), *Gram-Positive Pathogens*, 2nd ed, vol3. ASM Press, Washington, DC.
13. Lander GC, Tang L, Casjens S, Gilcrease EB, Prevelige PE, Poliakov A, Potter CS, Carragher B, Johnson JE. 2006. The structure of an infectious P22 virion shows the signal for headful DNA packaging. *Science* 312:1791–1795. <https://doi.org/10.1126/science.1127981>.
14. Schmieger H. 1982. Packaging signals for phage P22 on the chromosome of *Salmonella typhimurium*. *Mol Gen Genet* 187:516–518. <https://doi.org/10.1007/BF00332637>.
15. Fillol-Salom A, Bacigalupe R, Humphrey S, Chiang YN, Chen J, Penadés JR. 2021. Lateral transduction is inherent to the life cycle of the archetypical *Salmonella* phage P22. *Nat Commun* 12:6510. <https://doi.org/10.1038/s41467-021-26520-4>.
16. Kwoh DY, Kemper J. 1978. Bacteriophage P22-mediated specialized transduction in *Salmonella typhimurium*: high frequency of aberrant prophage excision. *J Virol* 27:519–534. <https://doi.org/10.1128/JVI.27.3.519-534.1978>.
17. Zahler SA, Korman RZ, Rosenthal R, Hemphill H. 1977. *Bacillus subtilis* bacteriophage SP β : localization of the prophage attachment site, and specialized transduction. *J Bacteriol* 129:556–558. <https://doi.org/10.1128/jb.129.1.556-558.1977>.
18. Kwoh DY, Kemper J. 1978. Bacteriophage P22-mediated specialized transduction in *Salmonella typhimurium*: identification of different types of specialized transducing particles. *J Virol* 27:535–550. <https://doi.org/10.1128/JVI.27.3.535-550.1978>.
19. Mackey CJ, Zahler SA. 1982. Insertion of bacteriophage SP beta into the *citF* gene of *Bacillus subtilis* and specialized transduction of the *ilvBC-leu* genes. *J Bacteriol* 151:1222–1229. <https://doi.org/10.1128/jb.151.3.1222-1229.1982>.
20. Cavenagh MM, Miller RV. 1986. Specialized transduction of *Pseudomonas aeruginosa* PAO by bacteriophage D3. *J Bacteriol* 165:448–452. <https://doi.org/10.1128/jb.165.2.448-452.1986>.
21. Hoppe I, Roth J. 1974. Specialized transducing phages derived from *salmonella* phage P22. *Genetics* 76:633–654. <https://doi.org/10.1093/genetics/76.4.633>.
22. Porter RD, Lark MW, Low KB. 1981. Specialized transduction with lambda plac5: dependence on *recA* and on configuration of *lac* and *att lambda*. *J Virol* 38:497–503. <https://doi.org/10.1128/JVI.38.2.497-503.1981>.
23. Campos J, Martínez E, Marrero K, Silva Y, Rodríguez BL, Suzarte E, Ledón T, Fando R. 2003. Novel Type of Specialized Transduction for CTX ϕ or Its Satellite Phage RS1 Mediated by Filamentous Phage VGJ ϕ in *Vibrio cholerae*. *J Bacteriol* 185:7231–7240. <https://doi.org/10.1128/JB.185.24.7231-7240.2003>.
24. Fink PS, Zahler SA. 1982. Specialized transduction of the *ilvD-thyB-ilvA* region mediated by *Bacillus subtilis* bacteriophage SP beta. *J Bacteriol* 150:1274–1279. <https://doi.org/10.1128/jb.150.3.1274-1279.1982>.
25. Porter RD, Welliver RA, Witkowski TA. 1982. Specialized transduction with lambda plac5: dependence on *recB*. *J Bacteriol* 150:1485–1488. <https://doi.org/10.1128/jb.150.3.1485-1488.1982>.
26. Kleiner M, Bushnell B, Sanderson KE, Hooper LV, Duerkop BA. 2020. Transductomics: sequencing-based detection and analysis of transduced DNA in pure cultures and microbial communities. *Microbiome* 8:158. <https://doi.org/10.1186/s40168-020-00935-5>.
27. Chiang YN, Penadés JR, Chen J. 2019. Genetic transduction by phages and chromosomal islands: the new and noncanonical. *PLoS Pathog* 15:e1007878. <https://doi.org/10.1371/journal.ppat.1007878>.
28. Fey PD, Endres JL, Yajjala VK, Widhelm TJ, Boissy RJ, Bose JL, Bayles KW. 2013. A genetic resource for rapid and comprehensive phenotype screening of nonessential *Staphylococcus aureus* genes. *mBio* 4:e00537-12. <https://doi.org/10.1128/mBio.00537-12>.
29. Lee CY, landolo JJ. 1988. Structural analysis of staphylococcal bacteriophage phi 11 attachment sites. *J Bacteriol* 170:2409–2411. <https://doi.org/10.1128/jb.170.5.2409-2411.1988>.
30. Goerke C, Pantucek R, Holtfreter S, Schulte B, Zink M, Grumann D, Bröcker BM, Doskar J, Wolz C. 2009. Diversity of prophages in dominant *Staphylococcus aureus* clonal lineages. *J Bacteriol* 191:3462–3468. <https://doi.org/10.1128/JB.01804-08>.
31. Campoy S, Hervàs A, Busquets N, Erill I, Teixidó L, Barbé J. 2006. Induction of the SOS response by bacteriophage lytic development in *Salmonella enterica*. *Virology* 351:360–367. <https://doi.org/10.1016/j.virol.2006.04.001>.
32. Ebel-Tsipis J, Fox MS, Botstein D. 1972. Generalized transduction by bacteriophage P22 in *Salmonella typhimurium*. II. Mechanism of integration of transducing DNA. *J Mol Biol* 71:449–469. [https://doi.org/10.1016/0022-2836\(72\)90362-2](https://doi.org/10.1016/0022-2836(72)90362-2).
33. Haaber J, Leisner JJ, Cohn MT, Catalan-Moreno A, Nielsen JB, Westh H, Penadés JR, Ingmer H. 2016. Bacterial viruses enable their host to acquire antibiotic resistance genes from neighbouring cells. *Nat Commun* 7:13333. <https://doi.org/10.1038/ncomms13333>.
34. Bae T, Class EM, Schneewind O, Missiakas D. 2007. Generating a collection of insertion mutations in the *Staphylococcus aureus* genome using bursa aurealis. *Methods Mol Biol* 416:103–116. https://doi.org/10.1007/978-1-59745-321-9_7.
35. Page AJ, De Silva N, Hunt M, Quail MA, Parkhill J, Harris SR, Otto TD, Keane JA. 2016. Robust high-throughput prokaryote de novo assembly and improvement pipeline for Illumina data. *Microb Genom* 2:e000083. <https://doi.org/10.1099/mgen.0.000083>.
36. Ponstingl H. 2016. SMALT – Wellcome Sanger Institute, <http://sourceforge.net/projects/smalt/>.
37. Carver T, Harris SR, Berriman M, Parkhill J, McQuillan JA. 2012. Artemis: an integrated platform for visualization and analysis of high-throughput sequence-based experimental data. *Bioinformatics* 28:464–469. <https://doi.org/10.1093/bioinformatics/btr703>.
38. Heringa S, Monroe J, Herrick J. 2007. A Simple, Rapid Method for Extracting Large Plasmid DNA from Bacteria. *Nat Prec* <https://doi.org/10.1038/npre.2007.1249.1>.